Contents lists available at ScienceDirect

Chemical Engineering Research and Design

journal homepage: www.elsevier.com/locate/cherd

Purification of crude wax using a filter medium modified with a nanofiber coating

Juliano Missau[a], *Juliana de Gregori da Rocha*[a], *Guilherme Luiz Dotto*[a], *Daniel Assumpção Bertuol*[a], *Luciano Peske Ceron*[b], *Eduardo Hiromitsu Tanabe*[a,*]

[a] *Environmental Processes Laboratory (LAPAM), Chemical Engineering Department, Federal University of Santa Maria — UFSM, Avenida Roraima 1000, 97105-900 Santa Maria, RS, Brazil*

[b] *Pontifícia Universidade Católica do Rio Grande do Sul — PUCRS, Engineering College, Chemical Engineering Department, Av. Ipiranga, 6681 Partenon, 90619-900 Porto Alegre, RS, Brazil*

ARTICLE INFO

Article history:
Received 11 July 2017
Received in revised form 14 May 2018
Accepted 21 June 2018
Available online 28 June 2018

Keywords:
Crude wax
Filter media coating
Nanofiber
Forcespinning®
Filtration

ABSTRACT

The presence of inorganic substances in the composition of crude wax decreases its commercial value, necessitating purification of the product. A new physical surface treatment for filter media involving the application of nanofibers of Nylon-6 polymer was developed using the Forcespinning® equipment. The performance of the nanofiber-coated filter was compared with the results obtained for other filter media of the same composition (nonwoven aramid fiber fabric), one without physical treatment, and another treated using singeing. An experimental design was carried out to find the optimum operating temperature and pressure (170 °C and 2.5 bar, respectively). The filtrate volume, specific resistance of the filter cake, and filter medium resistance were determined, keeping the filtration time, temperature, and pressure constant at 1 h, 170 °C, and 2.5 bar, respectively. The nanofiber-coated filter showed the best performance, providing a higher wax filtrate volume and greater retention of inorganics, with values of 5.39×10^{-5} m^3 and 99.6%, respectively.

1. Introduction

Plastics are durable, lightweight, and versatile, enabling their use in a diverse range of applications (Brems et al., 2013). An important group of plastics is the polyolefins. The advantages of this group include the facts that they are odorless, nontoxic, and offer good chemical resistance. The worldwide market for polypropylene (PP) is expected to reach 62.4 million metric tons by 2020 (Marek et al., 2015). The demand for plastics results in the generation of large quantities of plastic solid waste (PSW), which must be recycled for reasons that are both economic and environmental (Oyake-Ombis et al., 2015; Aznar et al., 2006). There are four main types of recycling processes, namely primary recycling (in-plant recycling), secondary recycling (mechanical recycling), tertiary recycling (chemical recycling), and quaternary recycling (energy recovery) (Wong et al., 2015). Chemical recycling can be achieved using techniques including pyrolysis, cracking, gasification, and chemolysis (Al-Salem et al., 2009).

Pyrolysis is a thermal decomposition process that occurs in the absence of oxygen. It is a promising option for the conversion of polymers into three major products: wax, oil, and gas (Lopez et al., 2017). These products are of value in the cosmetics, petrochemical, and other industries (Anuar Sharuddin et al., 2016; Almeida and Marques, 2015; Singhabhandhu and Tezuka, 2010). Pyrolysis does not cause contamination of water and is considered a green technology (Abnisa and Wan Daud, 2014). The process of production of high-density polyethylene, employing polymerization by addition of ethylene in reactors, is also a major source of paraffin wax (Cardoso and Fisch, 2016). There are many applications for wax. Synthetic wax can be used in applications as diverse as dietary markers in farm animals (Bachmann et al., 2016), modifiers of base bitumen (Merusi et al., 2017; Iwański et al., 2017), and temperature indicators for electrical connections in power distribution networks (Akishino et al., 2016). However, before they can be used, purification is required of the waxes obtained from the two processes mentioned above.

The purification of wax consists of the removal of inorganic substances that may be incorporated in it, as well as decoloration (Wiley-VCH, 2011). The crude wax purification technique usedin this

* *Corresponding author.*
E-mail address: edutanabe@ufsm.br (E.H. Tanabe).
https://doi.org/10.1016/j.cherd.2018.06.031

work was dead-end filtration under constant pressure, with the feed flow being forced perpendicularly through a filter medium that retained the impurities present in the wax, producing a filter cake and resulting in the outflow of a clarified fluid (Guan et al., 2017). The filter medium used was a nonwoven aramid fiber fabric (Kevlar). This was selected due to its good mechanical strength, thermal stability, and energy absorption properties (Li et al., 2014; Jackson and Samanta, 2015).

Different types of physical treatments have been developed with the aim of increasing the performance of materials, including coating (GPTMS/rGO) on AA-2024 aluminum alloy (Dun and Zuo, 2017), deposition of titanium coating on SiC fiber (Luo et al., 2017), boron nitride coatings on silicon carbide fibers (Yuan et al., 2016), and surface modification of aramid fibers with a hybrid coating (Chen et al., 2014). Other physical treatments that have been applied to filter media in order to increase filtration capacity include singeing, calendering, membrane coating, and laminating (Cirqueira et al., 2017; Qian et al., 2015). However, to the best of our knowledge, there have been no studies of the purification of crude waxes involving dead-end filtration and the use of filter media submitted to different types of physical treatments. The present work describes the coating of the filter medium with nanofibers produced by the Forcespinning® method (Sarkar et al., 2010). This equipment has been used previously to produce the following nanofibers: polyacrylonitrile (PAN) (Weng et al., 2014), poly(vinyl) butyral (PVB) (Weng et al., 2015a), Nylon-6 (Weng et al., 2015b), Sn/C composite (Agubra et al., 2016), and chitosan/polyamide (Dotto et al., 2017). Nylon-6 nanofibers were used here as a filter coating, due to their good thermal resistance (Weng et al., 2015b).

The objective of this work was therefore to develop a new physical treatment involving coating the filter with nanofibers. Different filter media (untreated, singed, and coated with nanofibers) were evaluated in the purification of crude wax. Firstly, the optimal parameters for the filtration process were determined using a central composite rotatable design (CCRD). Subsequently, Nylon-6 nanofibers produced by the Forcespinning® method were used to coat the filter medium. Finally, for each type of surface treatment, evaluation was made of the following filtration parameters: total volume of filtrate, specific resistance of the cake, and resistance of the filter medium.

2. Material and methods

2.1. Materials

Waste crude wax was kindly donated by the company Alkaest (Brazil). Perlite was obtained from Imerys (Argentina). Nylon-6 (Mw = 11,202) and formic acid (98%, HPLC grade) were purchased from Sigma–Aldrich. Filter media without and with physical treatment (singeing) were supplied by Renner Têxtil (Brazil).

2.2. Characterization of the materials

The solids content of the wax was measured by loss-on-ignition, using a muffle furnace (model 1109, Ind. Magnus, Brazil) operated at 500 °C for 2 h (Mu et al., 2017). The chemical groups present in the wax, the Nylon-6 nanofibers, and the filter media (untreated and coated) were identified by FTIR spectroscopy (IR Prestige 21, Shimadzu, Japan) (García et al., 2014). The viscosity of the wax was measured as a function of temperature, using a viscometer (VS/003, Brookfield, USA) (Goldstein, 1996). The specific mass of the crude wax was determined with a gas pycnometer (Ultrapyc 1200e, Quantachrome Corporation, USA) (Demers et al., 2014).

The grammages of the filter media were determined with a semi-analytical balance (model PB 303, Mettler Toledo, USA), following the NBR 12984:2009 standard procedure (Nonwoven — Determination of Mass per Unit Area). The filter thicknesses were measured with a thickness gauge (model M-73210-T, Mainard, Brazil), according to the NBR 13371:2005 procedure (Nonwoven — Determination of Thickness). The permeabilities of the filter media were determined with a permeability meter (model 6940, Karl Schroder KG, Germany), following the NBR 13706:1996 procedure (Nonwoven — Determination of Air Permeability).

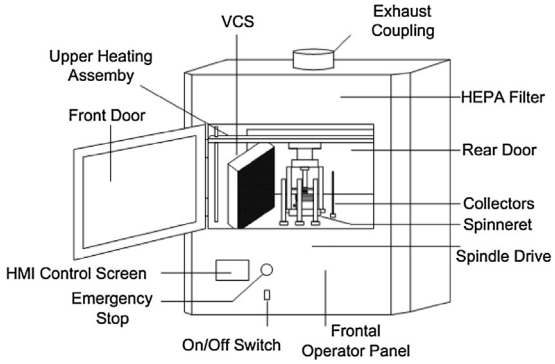

Fig. 1 – Schematic illustration of the Forcespinning® equipment used to produce the Nylon-6 nanofibers.

The morphological characteristics of the filter media and the Nylon-6 nanofibers were observed by scanning electron microscopy (SEM) (TESCAN, Czech Republic) (Goldstein et al., 2003). The mean nanofiber diameter was determined from the SEM micrographs using Image J software (NIH Image, USA) (Li et al., 2010). Thermogravimetric analysis (TGA) of the nanofibers was performed using a TGA-50 analyzer (Shimadzu, Japan) (Weng et al., 2015b).

2.3. Procedures

2.3.1. Preparation of Nylon-6 nanofibers and coating of filter media

Nylon-6 nanofibers were produced using a Forcespinning® system (model L1000-MS, FibeRio, USA), as shown in Fig. 1. A solution was prepared by dissolving 25 wt% of Nylon-6 in formic acid (98%) (Weng et al., 2015b). The Forcespinning® parameters (needle, rotational speed, % of maximum suction power in the vacuum creation system (VCS), collection time, and the spinneret solution/collection system distance) were set in order to produce a homogeneous nanofiber-coated filter. These parameters were based on previous studies (Weng et al., 2015b; Dotto et al., 2017), preliminary tests, and information provided by FibeRio. Approximately 2 mL of the solution was fed into the spinneret. Half-inch 30-gauge needles were connected to the spinneret solution. The equipment was operated for 9 min at a rotational speed of 10,000 rpm, with the fibers collected on equally spaced vertical steel pillars. Coating of the filter was achieved by attaching it to the VCS aligned with the collectors, which was operated at 75% of maximum suction power. The distance between the spinneret solution and the collection system (VCS equipment) was 12 cm.

2.3.2. Experimental apparatus and filtration experiments

The experiment apparatus used for the filter measurements is shown in Fig. 2. Firstly, the crude wax sample was quartered to ensure homogeneity (Mullin, 2001), followed by addition of approximately 3 wt% of perlite to the quartered wax (Purchas and Sutherland, 2002) and heating the mixture until it became fluid. The filter was positioned between the two flanges, with a metal screen placed on the lower flange as a support. Perlite was deposited on the filter, forming a 3 mm thick pre-coat

Table 1 – Experimental conditions of temperature (T) and pressure (P), according to the central composite design.

Assay	T (°C)[a]	P (bar)[a]
1	144.36 (−1)	1.44 (−1)
2	165.64 (1)	1.44 (−1)
3	144.36 (−1)	3.56 (1)
4	165.64 (1)	3.56 (1)
5	140 (−1.41)	2.5 (0)
6	170(1.41)	2.5 (0)
7	155 (0)	1.0 (−1.41)
8	155 (0)	4.0 (1.41)
9	155 (0)	2.5 (0)
10	155 (0)	2.5 (0)
11	155 (0)	2.5 (0)

[a] The coded values of the variables are in parentheses.

(Purchas and Sutherland, 2002). The apparatus was then connected to the bottom of the cylinder and the wax sample was fed to the top of the cylinder. After the system had reached thermal equilibrium, the cylinder was closed with the top cover and the nitrogen gas piping was connected. The pressure was maintained constant by controlling the nitrogen flow using a manometer (Dhabhai et al., 2016). The filtration time was measured from the moment when the first drop of filtrate appeared. Finally, the volume of filtered wax in the system was measured and the ash content of the product was determined.

2.3.3. *Experimental design*

A 2^2 central composite rotatable design (CCRD), with three central points and four axial points, was applied in order to obtain the optimal filtration conditions that provided the greatest amount of filtered wax. Three replicates at the center point were used to estimate the error sum of squares (Chielle et al., 2016; Myers et al., 2016). The experimental conditions, factors, and levels were established in preliminary tests and are presented in Table 1. The experimental design was generated using Statistica v. 10.0 software (Statsoft Inc.). The response variable was the total volume of filtered wax. In these tests, only the untreated filter medium was used. The filtration time was set at 10 min.

Table 2 – Operational conditions during the laboratory-scale liquid filtration tests.

ΔP (N/m²)	T (°C)	A (m²)	Cs (kg/m³)	μ (kg/m s)	ρ (g/cm³)
250000	170	4.71×10^{-4}	58.86	0.00195	0.9679

2.3.4. *Application of filter media with different physical surface treatments*

The different filter media were evaluated in terms of the volume of filtrate obtained, using the optimal temperature and pressure conditions determined from the experimental design. In this step, the filter media used were either untreated or physically treated (singed or coated with Nylon-6 nanofibers). The filtration time was 1 h. The specific resistance of the cake and the resistance of the filter medium were determined from Eq. (1), as used previously elsewhere (Sioutopoulos and Karabelas, 2016; Koch and Krammer, 2015; Mahdi and Holdich, 2013).

$$\frac{dt}{dV} = \frac{\mu\alpha C_s}{A^2(\Delta P)}V + \frac{\mu Rm}{A(\Delta P)} = K_p V + B \quad (1)$$

where V denotes the filtrate volume (m^3), A is the cross-sectional area of the filter (m^2), t is the filtration time (s), μ is the viscosity of the filtrate (Pa s), α is the specific cake resistance (m/kg), Rm is the resistance of the filter medium (m^{-1}), C_s is the solids concentration (kg solids/m^3 filtrate), and ΔP is the pressure drop across the filter (N/m^2). K_p (s/m^6) and B (s/m^3) are the filtration parameters. The operating conditions are listed in Table 2.

3. Results and discussion

3.1. *Characterization of the materials*

The loss-on-ignition test results showed that the impurities content of the crude wax was about 1.7%. These results were obtained as the average of ten analyses. The density of the crude wax was 0.9679 ± 0.003 g/cm³, obtained as the average of ten analyses using helium pycnometry.

Fig. 3 shows the Fourier transform infrared (FTIR) spectrum of the crude wax. The FTIR analysis enabled identification of the type of wax (linear or branched wax) to be purified

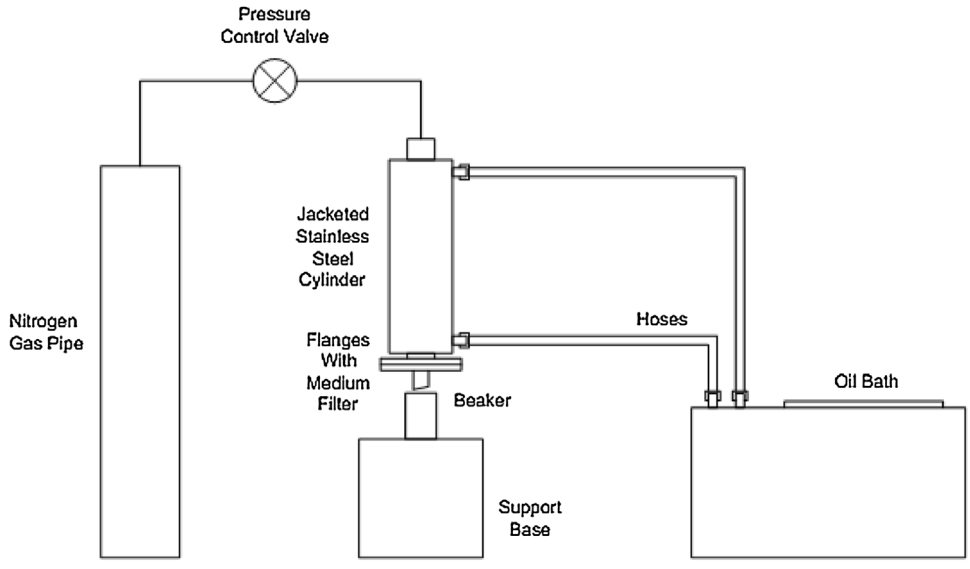

Fig. 2 – Schematic illustration of the filtration setup.

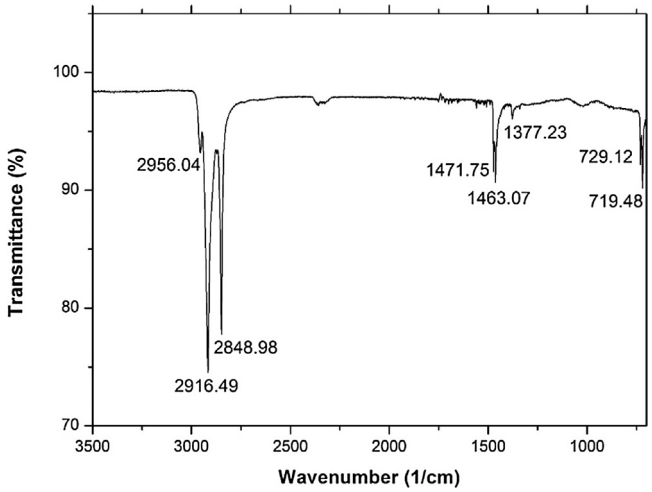

Fig. 3 – FTIR spectrum of the crude wax.

in this study (Silverstein et al., 2005). The results showed that the absorption frequencies were characteristic of normal alkanes, hence characterizing the crude wax as paraffin. The main characteristic vibrations of this class of compounds are due to the axial and angular deformations of C—H. The FTIR spectrum of the crude wax showed the following characteristic bands: 2956.04 cm^{-1} (asymmetric axial deformation of CH_3); 2916.49 cm^{-1} and 2848.98 cm^{-1} (symmetric axial deformations of CH_2); 1471.75 cm^{-1} and 1463.07 cm^{-1} (symmetric angular deformations of CH_2); 1377.23 cm^{-1} (symmetric angular deformation of CH_3); 729.12 cm^{-1} and 719.48 cm^{-1} (doublet asymmetric in-plane CH_2 deformations) (Silverstein et al., 2005).

Fig. 4 shows the TGA results for the Nylon-6 nanofibers. It can be seen from the TGA curve that the nanofibers started to degrade at around 380 °C, and were fully degraded below 480 °C. This analysis confirmed that the nanofibers were obtained from the Nylon-6 polymer, and also confirmed the high thermal resistance of these nanofibers (Weng et al., 2015b).

Fig. 5 shows SEM images of the surfaces of all the filter media (untreated, singed, and nanofiber-coated), revealing differences in the surfaces of the media. The fiber diameters were analyzed using Image J software.

It can be seen from Fig. 5(c) and (f) that in the case of the coated filter, the coating affected almost the entire filter surface, leading to greater uniformity of the fibers and fewer empty spaces, ensuring better coverage of the material with nanofibers. The images show that the nanofibers were long and homogeneous, but with some sites of agglomeration (Fig. 5(c)), which could have been due to the low viscosity of the solution (Zarrini et al., 2016).

The main characteristics of the filter media are provided in Table 3. The difference between the weights of the untreated filters and the filters coated with nanofibers was due to the mass of the deposited nanofibers. The nanofiber layer had a thickness of 0.20 mm and caused a decrease of 53.2% in the initial permeability, compared to the untreated filter, from 235 L/min dm^2 to 125 L/min dm^2.

The FTIR spectra of the Nylon-6 nanofibers and the filters (untreated and nanofiber-coated) are shown in Fig. 6. The nanofiber FTIR spectrum showed characteristic peaks of Nylon-6 at wavenumbers of 1543.12 cm^{-1} (N—H bending vibration, amide II), 1643.42 cm^{-1} (C=O stretching vibration, amide I), and 3305.17 cm^{-1} (N—H stretching vibration) (Weng et al., 2015b; Zarrini et al., 2016). The untreated filter medium exhibited absorption peaks at 3331.51 cm^{-1} (N—H stretching vibration), 1654.03 cm^{-1} (C=O stretching vibration, amide I), and 1548.91 cm^{-1} (coupling between C—N stretching vibration and N—H bending vibration) (Xu et al., 2016). Since nanofiber coating is a physical treatment that does not alter the chemical composition of the filter medium, the FTIR spectrum of the nanofiber-coated filter corresponded to the sum of the FTIR bands of the Nylon-6 nanofibers and the untreated filter medium.

3.2. *Statistical analysis*

The optimal filtration conditions were determined using the central composite rotatable design (CCRD). The effects of temperature (in the range from 140 to 170 °C) and pressure (in the range from 1 to 4 bar) were evaluated in order to obtain the maximum volume of filtered wax. The results for wax filtra-

Table 3 – Characteristics of the filtration media.

Surface treatment	Untreated	Singed	Nanofiber-coated
Average fiber diameter (μm)	11.68 ± 1.2	11.37 ± 1.69	0.592 ± 0.76
Grammage (g/m^2)	546	578	576
Thickness (mm)	2.8	2.6	3
Permeability (L/min dm^2)	235	130	125

Table 4 – Volumes of filtered wax obtained in experiments performed according to the CCRD model.

Assay	Filtered volume (cm^3)
1	5.21
2	8.23
3	8.65
4	8.57
5	6.66
6	13.27
7	5.67
8	8.14
9	5.51
10	4.45
11	5.08

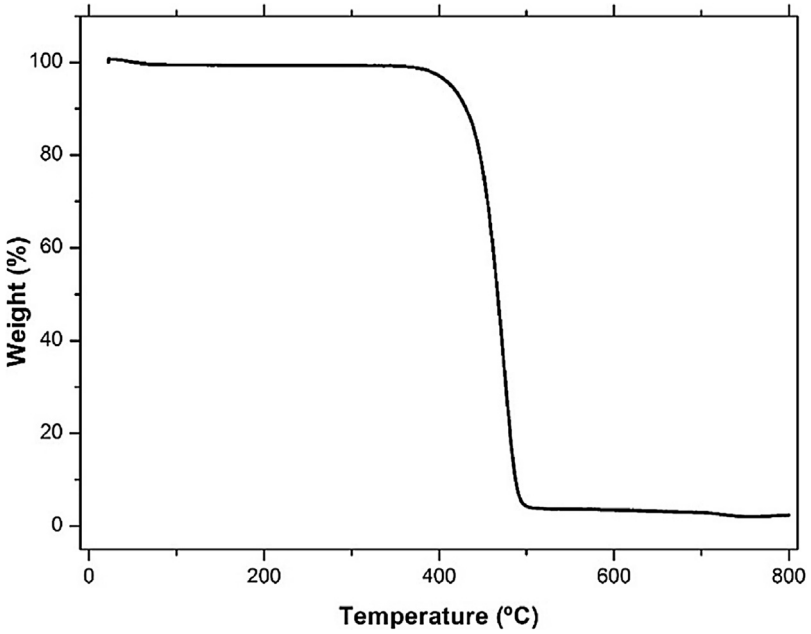

Fig. 4 – TGA curve for the Nylon-6 nanofibers.

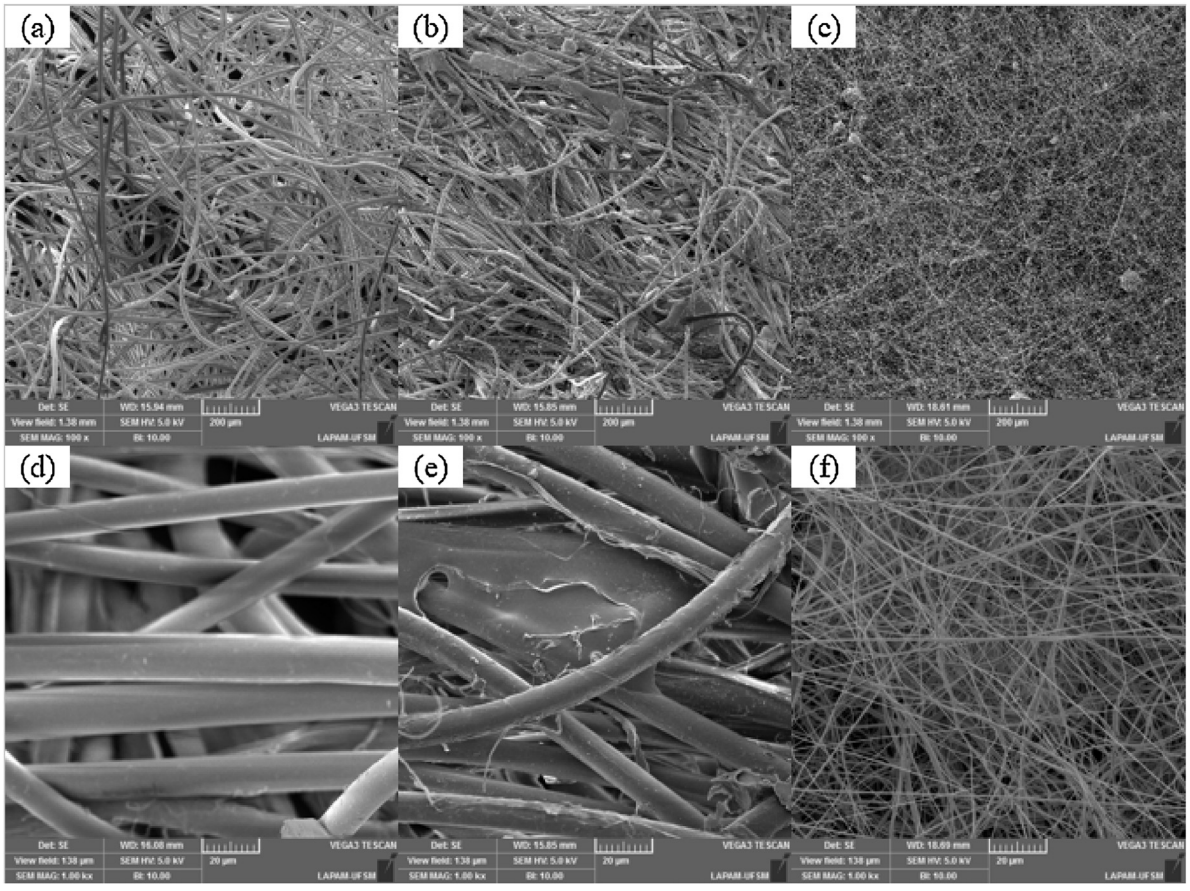

Fig. 5 – SEM images of the untreated (a), singed (b), and nanofiber-coated (c) filter media, at 100× magnification. Images (d), (e), and (f) are of the untreated, singed, and nanofiber-coated filter media, respectively, at a magnification of 1000×.

tion according to the CCRD are shown in Table 4 (Chielle et al., 2016).

Calculation of the regression coefficients (Table 5) was used to evaluate the significance of the effects of temperature and pressure on the volume of filtered wax. All the parameters evaluated were significant. The linear and quadratic effects of temperature and pressure were positively significant, while the interaction effect was negatively significant ($p < 0.10$).

The polynomial quadratic model for the dependence of the volume of filtered wax on T (coded value) and P (coded value) is shown in Eq. (2).

$$\text{Filtered volume} = 5.02 + 1.54T + 2.29T^2 + 0.91P + 0.75P^2 - 0.77\ TP \quad (2)$$

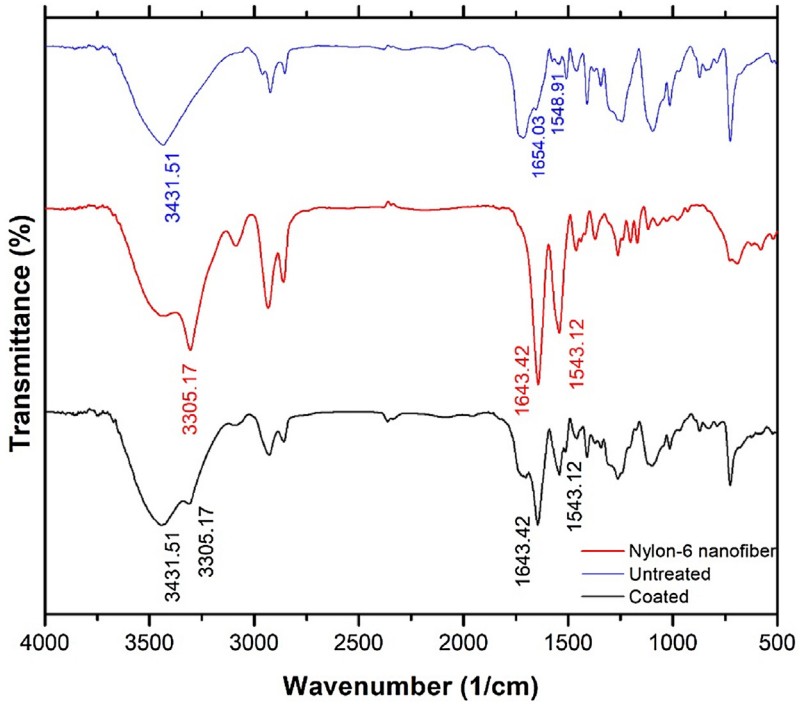

Fig. 6 – FTIR spectra of the Nylon-6 nanofibers and the untreated and coated filter media.

Table 5 – Regression coefficients for the effects of temperature and pressure on the volume of filtered wax.

Factor[a]	Regression coefficient	Standard error	t-test	p*
Mean	5.02	0.31	16.44	0.0037
Temperature (1) (°C) (L)	1.54	0.19	8.21	0.0145
Temperature (1) (°C) (Q)	2.29	0.22	10.26	0.0094
Pressure (2) (bar) (L)	0.91	0.19	4.87	0.0396
Pressure (2) (bar) (Q)	0.75	0.22	3.37	0.0781
1L by 2L	-0.77	0.26	-2.93	0.0996

[a] L = linear effect, Q = quadratic effect.
* Significance level of 90% ($p < 0.10$). If $p < 0.10$, the factor is significant.

Table 6 – ANOVA of the filtered volume of wax model at a 90% level of confidence.

Source of variation	Sum of squares	Degrees of freedom	Mean square	$F_{calc(90\%)}$	$F_{tab(90\%)}$	R^2
Regression	60.43	5	12.09	8.67	3.45	0.90
Residuals	6.97	5	1.39			
Lack of fit	6.41	3	2.14			
Pure error	0.56	2	0.28			
Total	64.28	10				

In order to satisfactorily represent the experimental data, the statistical model (Eq. (2)) should be predictive and significant (Myers et al., 2016). Therefore, analysis of residuals was also performed, which consisted of a significance test of the model fit based on analysis of variance (ANOVA), calculation of the coefficient of determination (R^2), and the F-test. The results obtained were predictive at the 90% confidence limit, since the calculated F value (8.67) was higher than the tabulated F value (3.45), as shown in Table 6.

Table 7 – Variation of the viscosity of the crude wax as a function of temperature.

Temperature (°C)	Viscosity (cp)
130	29 ± 0.35
140	3.45 ± 0.15
150	3.15 ± 0.3
160	2.00 ± 0.45
170	1.95 ± 0.15

Since the model was statistically valid, Eq. (2) was used to generate a response surface (Fig. 7) showing the volume of filtered wax as a function of the independent variables (temperature and pressure).

The temperature was the parameter that showed the greatest significance. The best temperature was around 170 °C, due to the fact that the higher the temperature, the lower the viscosity of the wax (Shames, 2002), enabling the wax to pass more easily through the filter medium. This behavior was confirmed by analysis of the viscosity of the wax as a function of temperature (Table 7), as well as by the experimental volumes of filtered wax (Table 4). At constant pressure (2.5 bar), the filtered volume of wax increased from 6.66 to 13.27 cm^3, when the temperature was increased from 140 to 170 °C.

The effect of pressure was not as significant as that of temperature. Studies have shown that the same filter media may exhibit differences in terms of filtration rate and clarification of the filtrate (Koch and Krammer, 2015), which could be caused by partial blockage of the filter medium by solid particles soon after the start of the filtration process. This effect can be significant, even in the case of perfectly homogeneous filters. As a result, the effect of pressure is of greater significance during the initial stages of the filtration, before complete formation of the cake (Roussel et al., 2007). Based on the results, the pressure chosen was 2.5 bar, since higher pressures would lead to wastage of nitrogen and increased cost of the wax filtration.

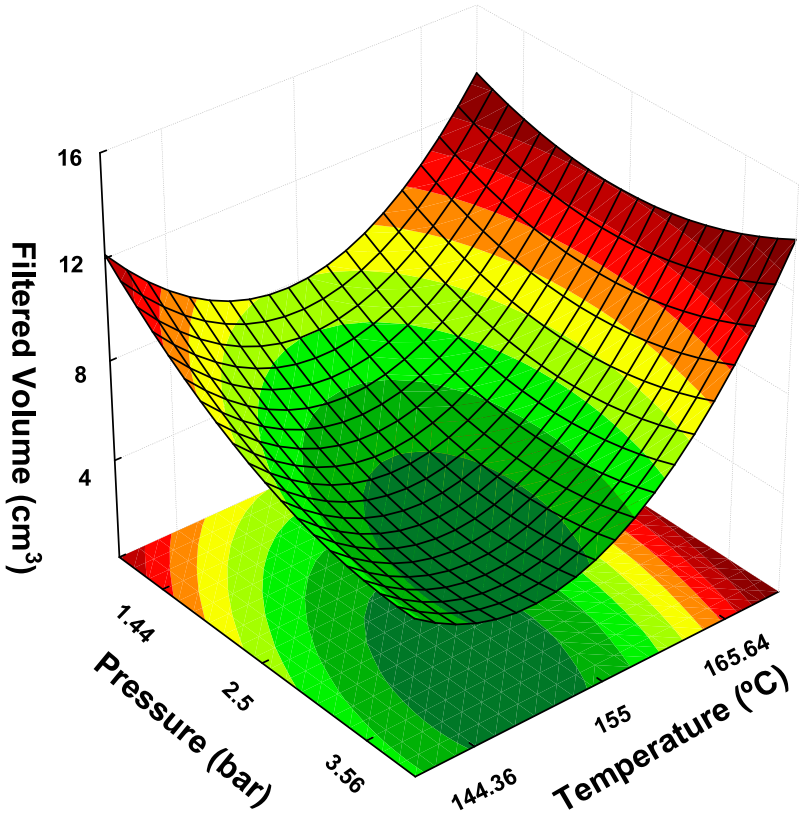

Fig. 7 – Response surface for the volume of filtered wax as a function of temperature and pressure.

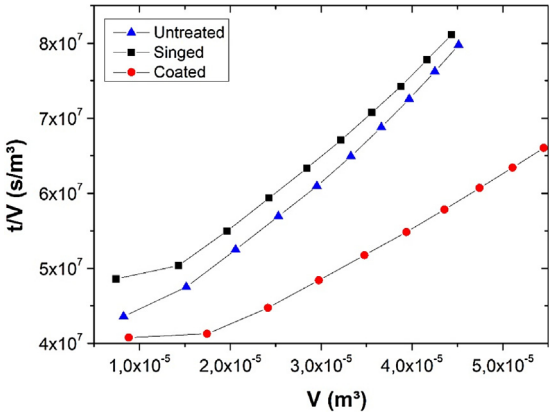

Fig. 8 – Plots of t/V against V for the filtration tests performed with an untreated filter (blue triangles), a singed filter (black squares), and a nanofiber-coated filter (red circles). (For interpretation of the references to colour in this figure legend, the reader is referred to the web version of this article.)

Therefore, the best conditions chosen for maximizing the volume of filtered wax were a temperature of 170 °C and a pressure of 2.5 bar, which were employed in the subsequent filtration tests.

3.3. *Filtration tests*

Fig. 8 shows the results of the filtration tests, in the form of filtration curves obtained by plotting the experimental t/V values against V. A filtration time of 60 min was used for each type of filter medium: untreated (blue triangles), singed (black squares), and nanofiber-coated (red circles). The filtration tests were performed in triplicate, but for clarity, only one of the curves for each filter medium is presented. The results demonstrated that coating the filter surface with Nylon-6 nanofibers increased the volume of filtered wax.

Table 8 – Mean values of the variables in the filtration experiments, obtained by plotting the volume versus time/volume curves for each type of filter medium, and the average values of the specific resistance of the cake and the resistance of the filter medium.

Surface treatment	Untreated	Singed	Nanofiber-coated
$V^{*}10^{-5}$ (m^3)	4.54	4.49	5.39
$Kp^{*}10^{12}$ ($s\,m^{-6}$)	2.17	1.76	1.26
$B^{*}10^{7}$ ($s\,m^{-3}$)	2.92	3.87	3.39
$\alpha^{*}10^{12}$ ($m\,kg^{-1}$)	10.50	8.50	6.09
$Rm^{*}10^{12}$ (m^{-1})	1.79	2.34	2.05

Table 8 presents the mean values of the variables obtained during the filtration experiments. Use of the nanofiber-coated filter medium resulted in the greatest volume of filtered wax of $5.39 \times 10^{-5}\,m^3$, which was 17% higher than obtained for the singed filter. The filtration parameters (Kp and B) were obtained by fitting the curves shown in Fig. 8 (Geankoplis, 1993). Use of the coated filter medium resulted in the lowest value for the specific resistance of the cake ($6.09 \times 10^{12}\,m\,kg^{-1}$). The resistance of the coated medium was $2.05 \times 10^{12}\,m^{-1}$, an intermediate value when compared to the values reported for other filter media submitted to different types of physical treatments.

Despite having a lower permeability (Table 3), the nanofiber-coated filter resulted in the highest volume of filtered wax, which was probably because the 0.20 mm thick layer of Nylon-6 nanofibers acted as a filtration aid (together with the 3 mm thick pre-coat of perlite). Consequently, the nanofiber-coated filter could increase the porosity of the cake on the surface of the filter medium. These findings were in

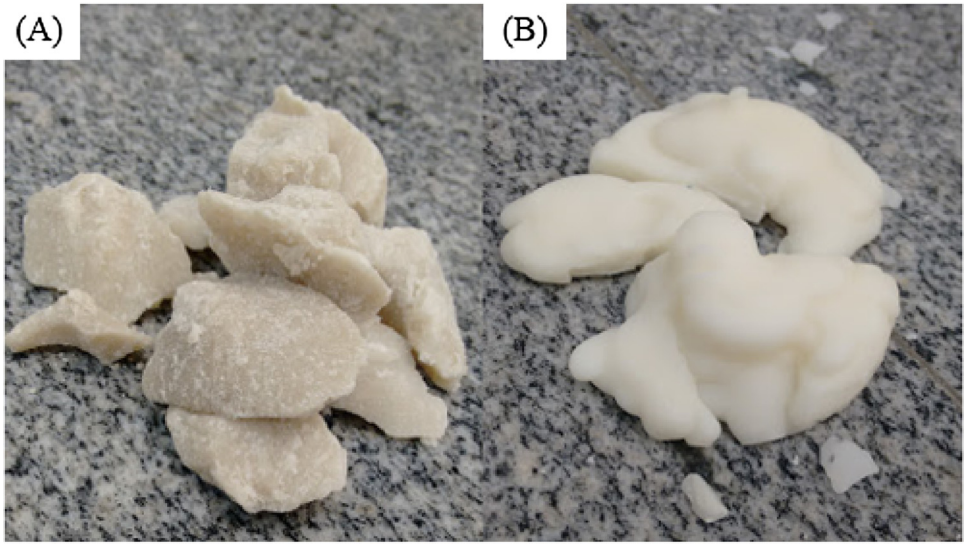

Fig. 9 – Images of the crude wax (A) before and (B) after the filtration process.

Table 9 – Mean contents of inorganics, determined using loss-on-ignition analysis, and the solids removal percentages, for each type of filter medium during filtration for 60 min.

Wax sample	Inorganics content (g)	Removal percentage
Crude wax	0.0850 ± 0.005	
Filtered wax (untreated filter)	0.0007 ± 0.0001	99.21
Filtered wax (singed filter)	0.0005 ± 0.00005	99.41
Filtered wax (coated filter)	0.0003 ± 0.00005	99.60

agreement with the fact that the lowest specific resistance of the filter cake was obtained with the nanofiber-coated filters (Table 8). Khude (2017) reported that the presence of nanofibers provided higher filter efficiency and a high filtration volume, with relatively small decreases in permeability. Other studies have also described the use of filtration aids to facilitate the filtrate flow, increase cake porosity, and provide a higher volume of filtrate (Du et al., 2011; Lee and Eiteman, 2001).

The percentage removal of inorganic content exceeded 99% for the 3 types of filter medium tested (Table 9), with the greatest removal (99.6%) achieved with the nanofiber-coated medium. This could be explained by the presence of fewer voids on the surface of the medium, which also resulted in lower permeability (Table 3) (Sinha-Ray et al., 2015). Hence, a greater contact surface area was available for the retention of impurities. All the experiments were performed under identical operating conditions, and in all cases, the filtration resulted in the removal of the color of the crude wax, leaving it whitish in color (Fig. 9).

The results demonstrated that the most effective physical surface treatment was coating with Nylon-6 nanofibers. This treatment resulted in a greater volume of filtered wax and a higher degree of purification.

4. Conclusions

The Nylon-6 nanofibers produced with the Forcespinning® equipment were long and homogeneous, and presented high thermal resistance. The optimal conditions for the filtration experiments, determined using experimental design, were a temperature of 170 °C and pressure of 2.5 bar. Comparison of the use of untreated, singed, and nanofiber-coated filter media for the filtration of crude wax confirmed the superior performance of the nanofiber-coated filter medium, with a filtered volume of wax of 5.39×10^{-5} m^3 and 99.6% retention of impurities. The physical treatment of filter media by coating with nanofibers is a promising technology that could be employed in larger-scale trials to evaluate potential applications of these systems.

Acknowledgments

The authors would like to thank CAPES (Brazilian Agency for Improvement of Graduate Personnel), CNPq (National Council of Scientific and Technological Development), FAPERGS (Foundation for Research Support of the State of Rio Grande do Sul), and SDECT (Department of Economic Development, Science and Technology of the State of Rio Grande do Sul) for financial support.

References

Abnisa, F., Wan Daud, W.M.A., 2014. A review on co-pyrolysis of biomass: an optional technique to obtain a high-grade pyrolysis oil. Energy Convers. Manag. 87, 71–85, http://dx.doi.org/10.1016/j.enconman.2014.07.007.

Agubra, V.A., Zuniga, L., La Garza, D., De Gallegos, L., Pokhrel, M., Alcoutlabi, M., 2016. Forcespinning: a new method for the mass production of Sn/C composite nanofiber anodes for lithium ion batteries. Solid State Ionics 286, 72–82, http://dx.doi.org/10.1016/j.ssi.2015.12.020.

Akishino, J.K., Cerqueira, D.P., Silva, G.C., Swinka-Filho, V., Munaro, M., 2016. Morphological and thermal evaluation of blends of polyethylene wax and paraffin. Thermochim. Acta 626, 9–12, http://dx.doi.org/10.1016/j.tca.2016.01.002.

Al-Salem, S.M., Lettieri, P., Baeyens, J., 2009. Recycling and recovery routes of plastic solid waste (PSW): a review. Waste Manag. 29, 2625–2643, http://dx.doi.org/10.1016/j.wasman.2009.06.004.

Almeida, D., Marques, M.F., 2015. Thermal and catalytic pyrolysis of plastic waste. Polimeros 26, 1–8, http://dx.doi.org/10.1590/0104-1428.2100.

Anuar Sharuddin, S.D., Abnisa, F., Wan Daud, W.M.A., Aroua, M.K., 2016. A review on pyrolysis of plastic wastes. Energy

Convers. Manag. 115, 308–326, http://dx.doi.org/10.1016/j.enconman.2016.02.037.
Aznar, P., Caballero, M.A., Sancho, A., France, E., 2006. Plastic waste elimination by co-gasification with coal and biomass in fluidized bed with air in pilot plant. Fuel Process. Technol. 87, 409–420, http://dx.doi.org/10.1016/j.fuproc.2005.09.006.
Bachmann, M., Wensch-Dorendorf, M., Mäder, K., Bulang, M., Zeyner, A., 2016. Preparation of synthetic alkane waxes and investigations on their suitability for application as dietary markers in farm animals. Livest. Sci. 185, 110–116, http://dx.doi.org/10.1016/j.livsci.2016.01.018.
Brems, A., Dewil, R., Baeyens, J., Zhang, R., 2013. Gasification of plastic waste as waste-to-energy or waste-to-syngas recovery route. Nat. Sci. 05, 695–704, http://dx.doi.org/10.4236/ns.2013.56086.
Cardoso, M.N., Fisch, A.G., 2016. Mechanism of fouling in slurry polymerization reactors of olefins. Ind. Eng. Chem. Res. 55, 9426–9432, http://dx.doi.org/10.1021/acs.iecr.6b02490.
Chen, J., Zhu, Y., Ni, Q., Fu, Y., Fu, X., 2014. Surface modification and characterization of aramid fibers with hybrid coating. Appl. Surf. Sci. 321, 103–108, http://dx.doi.org/10.1016/j.apsusc.2014.09.196.
Chielle, D.P., Bertuol, D.A., Meili, L., Tanabe, E.H., Dotto, G.L., 2016. Convective drying of papaya seeds (*Carica papaya* L.) and optimization of oil extraction. Ind. Crops Prod. 85, 221–228, http://dx.doi.org/10.1016/j.indcrop.2016.03.010.
Cirqueira, S.S.R., Tanabe, E.H., Aguiar, M.L., 2017. Evaluation of operating conditions during the pulse jet cleaning filtration using different surface treated fibrous filters. Process Saf. Environ. Prot. 105, 69–78, http://dx.doi.org/10.1016/j.psep.2016.10.010.
Demers, V., Turenne, S., Scalzo, O., 2014. Segregation measurement of powder injection molding feedstock using thermogravimetric analysis, pycnometer density and differential scanning calorimetry techniques. Adv. Powder Technol. 26, 997–1004, http://dx.doi.org/10.1016/j.apt.2015.04.005.
Dhabhai, R., Ahmadifeijani, E., Dalai, A.K., Reaney, M., 2016. Purification of crude glycerol using a sequential physico-chemical treatment, membrane filtration, and activated charcoal adsorption. Sep. Purif. Technol. 168, 101–106, http://dx.doi.org/10.1016/j.seppur.2016.05.030.
Dotto, G.L., Santos, J.M.N., Tanabe, E.H., Bertuol, D.A., Foletto, E.L., Lima, E.C., Pavan, F.A., 2017. Chitosan/polyamide nanofibers prepared by Forcespinning® technology: a new adsorbent to remove anionic dyes from aqueous solutions. J. Clean. Prod. 144, 120–129, http://dx.doi.org/10.1016/j.jclepro.2017.01.004.
Du, L., Chen, X., Li, W., Zhu, Q., 2011. A study on enhancement of filtration process with filter aids diatomaceous earth and wood pulp cellulose. Chin. J. Chem. Eng. 19, 792–798, http://dx.doi.org/10.1016/S1004-9541(11)60058-X.
Dun, Y., Zuo, Y., 2017. Preparation and characterization of a GPTMS/graphene coating on AA-2024 alloy. Appl. Surf. Sci. 416, 492–502, http://dx.doi.org/10.1016/j.electacta.2010.01.041.
García, G.B., Calero De Hoces, M., Martínez García, C., Cotes Palomino, M.T., Gálvez, A.R., Martín-Lara, M.Á., 2014. Characterization and modeling of pyrolysis of the two-phase olive mill solid waste. Fuel Process. Technol. 126, 104–111, http://dx.doi.org/10.1016/j.fuproc.2014.04.020.
Geankoplis, C.J., 1993. Transport Processes and Unit Operations. Prentice-Hall Int.
Goldstein, R.J., 1996. Fluid Mechanics Measurements, 2nd ed. CRC Press.
Goldstein, J., Newbury, D.E., Joy, D.C., Lyman, C.E., Echlin, P., Lifshin, E., Sawyer, L., Michael, J.R., 2003. Scanning Electron Microscopy and X-ray Microanalysis, Third Edit3rd ed. Springer US.
Guan, K., Liu, Y., Yin, X., Zhu, W., Chu, Y., Peng, C., Lv, M., Sun, Q., Rao, P., Wu, J., Carlo, M., 2017. Influence of operation conditions on cake structure in dead-end membrane filtration: Monte Carlo simulations and a force model. Chem. Eng. Res. Des. 124, 124–133, http://dx.doi.org/10.1016/j.cherd.2017.06.008.
Iwański, M., Mrugała, J., Chomicz-Kowalska, A., 2017. Optimization of composition of asphalt concrete with synthetic wax modified foamed bitumen in scope of resistance to climatic conditions. Procedia Eng. 172, 409–416, http://dx.doi.org/10.1016/j.proeng.2017.02.008.
Jackson, T., Samanta, S., 2015. Characterization of Kevlar fiber and its composites: a review. Mater. Today Proc. 2, 1381–1387, http://dx.doi.org/10.1016/j.matpr.2015.07.057.
Koch, M., Krammer, G., 2015. Permeability distribution for filter media characterization in solid liquid filtration. Powder Technol. 271, 182–186, http://dx.doi.org/10.1016/j.powtec.2014.10.042.
Khude, P., 2017. Nanofibers for High Efficiency Filtration. J. Mater. Sci. Eng., 1–10, http://dx.doi.org/10.4172/2169-0022.1000399.
Lee, S.A., Eiteman, M.A., 2001. Ground kenaf core as a filtration aid. Ind. Crops Prod. 13, 155–161, http://dx.doi.org/10.1016/S0926-6690(00)00062-5.
Li, X., Anton, N., Arpagaus, C., Belleteix, F., Vandamme, T.F., 2010. Nanoparticles by spray drying using innovative new technology: the Buchi Nano Spray Dryer B-90. J. Control. Release 147, 304–310, http://dx.doi.org/10.1016/j.jconrel.2010.07.113.
Li, T., Wang, R., Lou, C., Lin, J., 2014. Static and dynamic puncture behaviors of compound fabrics with recycled high-performance Kevlar fibers. Composites B 59, 60–66, http://dx.doi.org/10.1016/j.compositesb.2013.10.063.
Lopez, G., Artetxe, M., Amutio, M., Bilbao, J., Olazar, M., 2017. Thermochemical routes for the valorization of waste polyolefinic plastics to produce fuels and chemicals. A review. Renew. Sustain. Energy Rev. 73, 346–368, http://dx.doi.org/10.1016/j.rser.2017.01.142.
Luo, X., Wu, S., Yang, Y., Jin, Qing, Liu, N., Huang, S., 2017. Deposition of titanium coating on SiC fiber by chemical vapor deposition with Ti–I_2 system. Appl. Surf. Sci. 406, 62–68, http://dx.doi.org/10.1016/j.matchemphys.2016.09.041.
Mahdi, F.M., Holdich, R.G., 2013. Laboratory cake filtration testing using constant rate. Chem. Eng. Res. Des. 91, 1145–1154, http://dx.doi.org/10.1016/j.cherd.2012.11.012.
Marek, A.A., Zawadiak, J., Piotrowski, T., Hefczyc, B., 2015. A new efficient method for the processing of post-consumer polypropylene and other polyolefin wastes into polar waxes. Waste Manag. 46, 62–67, http://dx.doi.org/10.1016/j.wasman.2015.08.042.
Merusi, F., Filippi, S., Polacco, G., 2017. Effect of synthetic and functionalized waxes on bituminous binders: from the glassy state to the intermediate viscoelastic domain. Constr. Build. Mater. 136, 541–555, http://dx.doi.org/10.1016/j.conbuildmat.2017.01.062.
Mu, Y., Saffarzadeh, A., Shimaoka, T., 2017. Influence of ignition process on mineral phase transformation in municipal solid waste incineration (MSWI) fly ash: implications for estimating loss-on-ignition (LOI). Waste Manag. 59, 222–228, http://dx.doi.org/10.1016/j.wasman.2016.09.028.
Mullin, W.J., 2001. Crystallization, 4th ed. Butterworth-Heinemann.
Myers, R.H., Montgomery, D.C., Anderson-Cook, C.M., 2016. Response Surface Methodology: Process and Product Optimization Using Designed Experiments. Wiley.
Oyake-Ombis, L., van Vliet, B.J.M., Mol, A.P.J., 2015. Managing plastic waste in East Africa: niche innovations in plastic production and solid waste. Habitat Int. 48, 188–197, http://dx.doi.org/10.1016/j.habitatint.2015.03.019.
Purchas, D.B., Sutherland, K., 2002. Handbook of Filter Media, 2nd ed. Elsevier Science.
Qian, Y., Bi, Y., Zhang, M., Chen, H., Xu, G., 2015. Effect of filtration operation and surface treatment on pulse-jet cleaning performance of filter bags. Powder Technol. 277, 82–88, http://dx.doi.org/10.1016/j.powtec.2015.02.036.
Roussel, N., Nguyen, T.L.H., Coussot, P., 2007. General probabilistic approach to the filtration process. Phys. Rev. Lett. 98 (1–4), 114502, http://dx.doi.org/10.1103/PhysRevLett.98.114502.
Sarkar, K., Gomez, C., Zambrano, S., Ramirez, M., De Hoyos, E., Vasquez, H., Lozano, K., 2010. Electrospinning to

forcespinning. Mater. Today 13, 12–14, http://dx.doi.org/10.1016/S1369-7021(10)70199-1.
Shames, I.H., 2002. Mechanics of Fluids (Mcgraw-Hill Series in Mechanical Engineering), 4th ed. Mcgraw-Hill, TX.
Silverstein, R.M., Webster, F.X., Kiemle, D.J., 2005. Spectrometric Identification of Organic Compounds, 7th ed. John Wiley & Sons, Inc.
Singhabhandhu, A., Tezuka, T., 2010. The waste-to-energy framework for integrated multi-waste utilization: waste cooking oil, waste lubricating oil, and waste plastics. Energy 35, 2544–2551, http://dx.doi.org/10.1016/j.energy.2010.03.001.
Sinha-Ray, S., Sinha-Ray, S., Yarin, A.L., Pourdeyhimi, B., 2015. Application of solution-blown 20–50 nm nanofibers in filtration of nanoparticles: the efficient van der Waals collectors. J. Membr. Sci. 485, 132–150, http://dx.doi.org/10.1016/j.memsci.2015.02.026.
Sioutopoulos, D.C., Karabelas, A.J., 2016. Evolution of organic gel fouling resistance in constant pressure and constant flux dead-end ultrafiltration: differences and similarities. J. Membr. Sci. 511, 265–277, http://dx.doi.org/10.1016/j.memsci.2016.03.057.
Weng, B., Xu, F., Lozano, K., 2014. Mass production of carbon nanotube-reinforced polyacrylonitrile fine composite fibers. J. Appl. Polym. Sci. 131, 1–9, http://dx.doi.org/10.1002/app.40302.
Weng, B., Xu, F., Garza, G., Alcoutlabi, M., Salinas, A., Lozano, K., 2015a. The production of carbon nanotube reinforced poly(vinyl) butyral nanofibers by the forcespinningVR method. Polym. Eng. Sci., 81–87, http://dx.doi.org/10.1002/pen.23872.
Weng, B., Xu, F., Lozano, K., 2015b. Development of hierarchical structured carbon nanotube-nylon nanofiber mats. J. Appl. Polym. Sci. 132, 1–7, http://dx.doi.org/10.1002/app.42535.
Wiley-VCH, 2011. Ullmann's Encyclopedia of Industrial Chemistry, 1st ed. John Wiley Reference.
Wong, S.L., Ngadi, N., Abdullah, T.A.T., Inuwa, I.M., 2015. Current state and future prospects of plastic waste as source of fuel: a review. Renew. Sustain. Energy Rev. 50, 1167–1180, http://dx.doi.org/10.1016/j.rser.2015.04.063.
Xu, F., Fan, W., Zhang, Y., Gao, Y., Jia, Z., Qiu, Y., Hui, D., 2016. Modification of tensile, wear and interfacial properties of Kevlar fibers under cryogenic treatment. Composites B, 1–8, http://dx.doi.org/10.1016/j.compositesb.2016.10.082.
Yuan, M., Zhou, T., He, J., Chen, L., 2016. Formation of boron nitride coatings on silicon carbide fibers using trimethylborate vapor. Appl. Surf. Sci. 382, 27–33, http://dx.doi.org/10.1016/j.apsusc.2016.04.080.
Zarrini, K., Rahimi, A.A., Alihosseini, F., Fashandi, H., 2016. Highly efficient dye adsorbent based on polyaniline-coated nylon-6 nanofibers. J. Clean. Prod. 142, 3645–3654, http://dx.doi.org/10.1016/j.jclepro.2016.10.103.